

***Electronic Supplementary Information***

**Influence of picolinate ancillary ligands on unique photophysical properties  
of Ir(ppz)<sub>2</sub>(LX)**

Daehoon Kim,<sup>a</sup> Mina Ahn,<sup>a</sup> Kyung-Ryang Wee,<sup>a,\*</sup> Dae Won Cho<sup>b,c\*</sup>

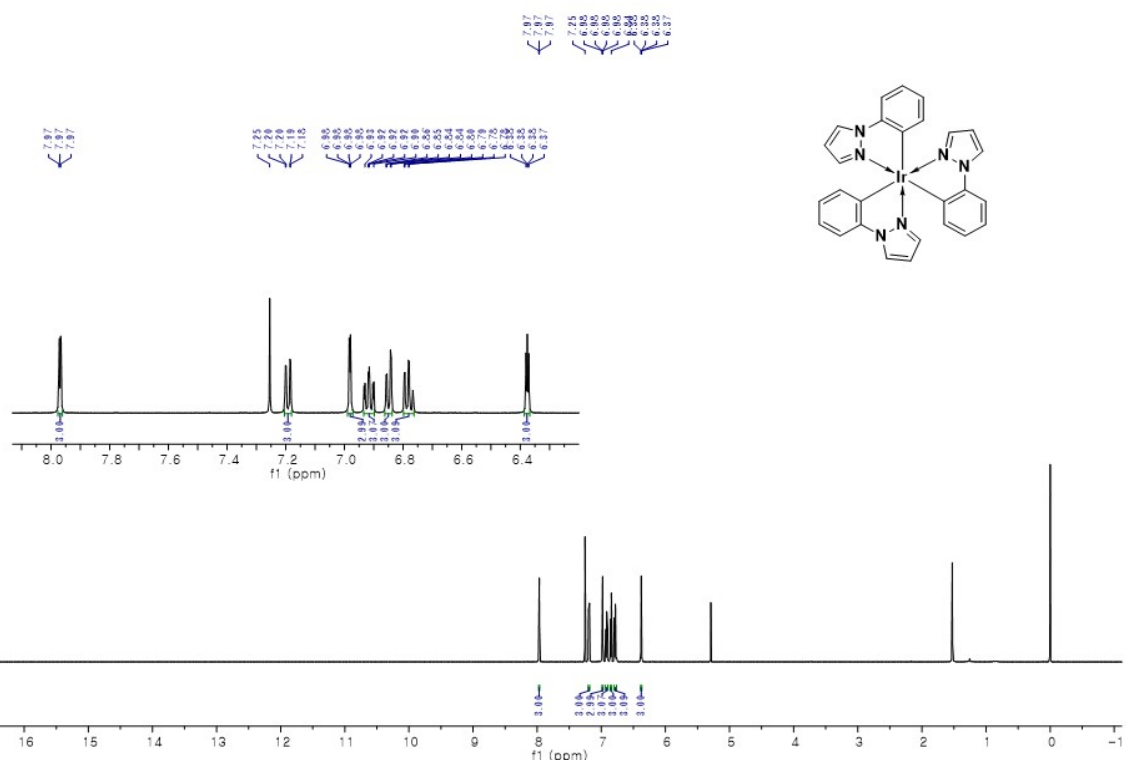
a. Department of Chemistry, Daegu University, Gyeongsan 38453, Republic of Korea

b. Center for Photovoltaic Materials, Korea University, Sejong Campus, Sejong 30019, Korea

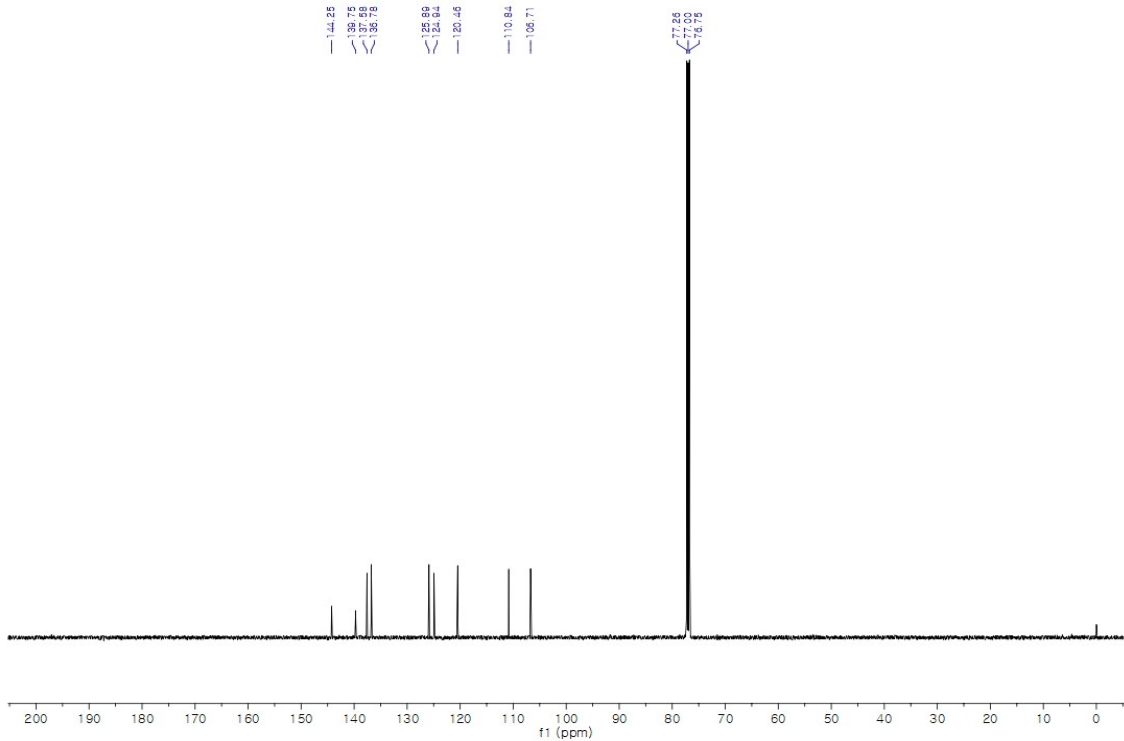
c. Present address: Center for Advanced Reaction Dynamics, Institute for Basic Science, Daejeon 34141, Republic of Korea

**Contents**

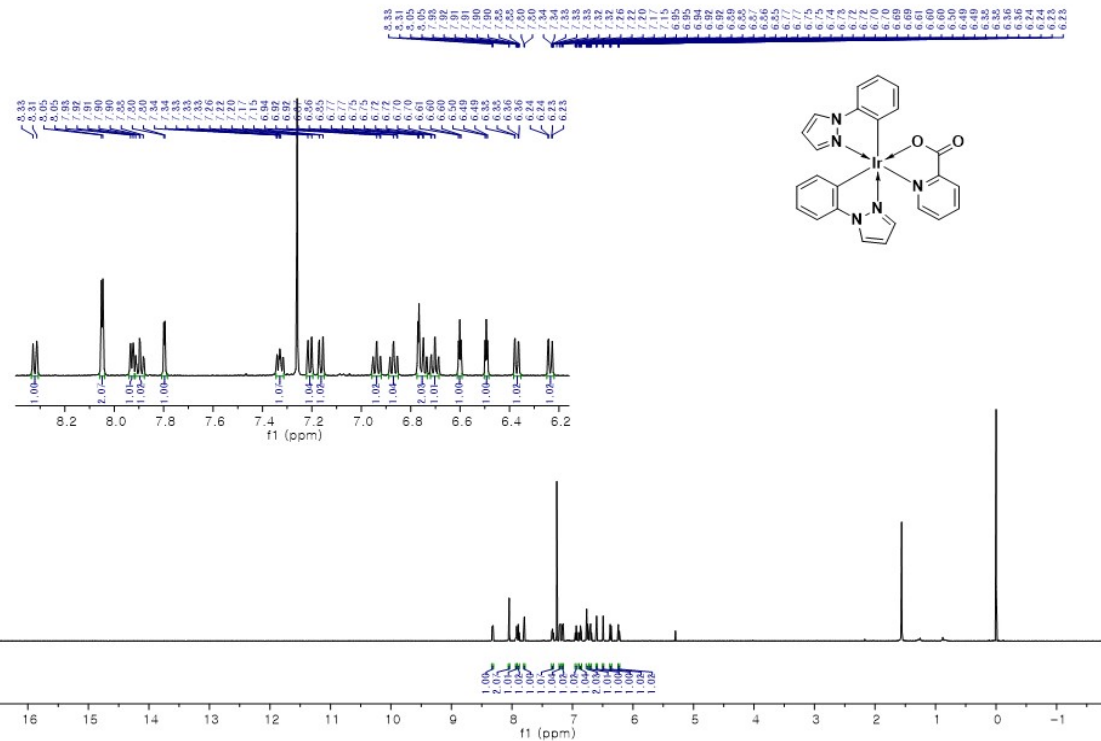
- 
- Fig. S1-S8. <sup>1</sup>H-NMR and <sup>13</sup>C-NMR spectra of Ir(ppz)<sub>3</sub> and Ir(ppz)<sub>2</sub>(LX)
  - Fig. S9. GC-MS data of Ir(ppz)<sub>3</sub> and Ir(ppz)<sub>2</sub>(LX)
  - Fig. S10-S12. DFT calculation: Energy levels and isodensity plot
  - Fig. S13. Emission decay profiles in glassy MTHF matrix at 77K
  - Fig. S14. TA spectra of Ir(ppz)<sub>2</sub>(picOH) in the CH<sub>2</sub>Cl<sub>2</sub>-ethanol (v/v = 2:8)
  - Table S1-S4. DFT calculation: Cartesian coordinates for optimized structure
  - Fig. S15-S18. TD-DFT calculation: Electronic transition and simulated spectra
  - Table S5-S8. TD-DFT calculation: Transition assignment
-



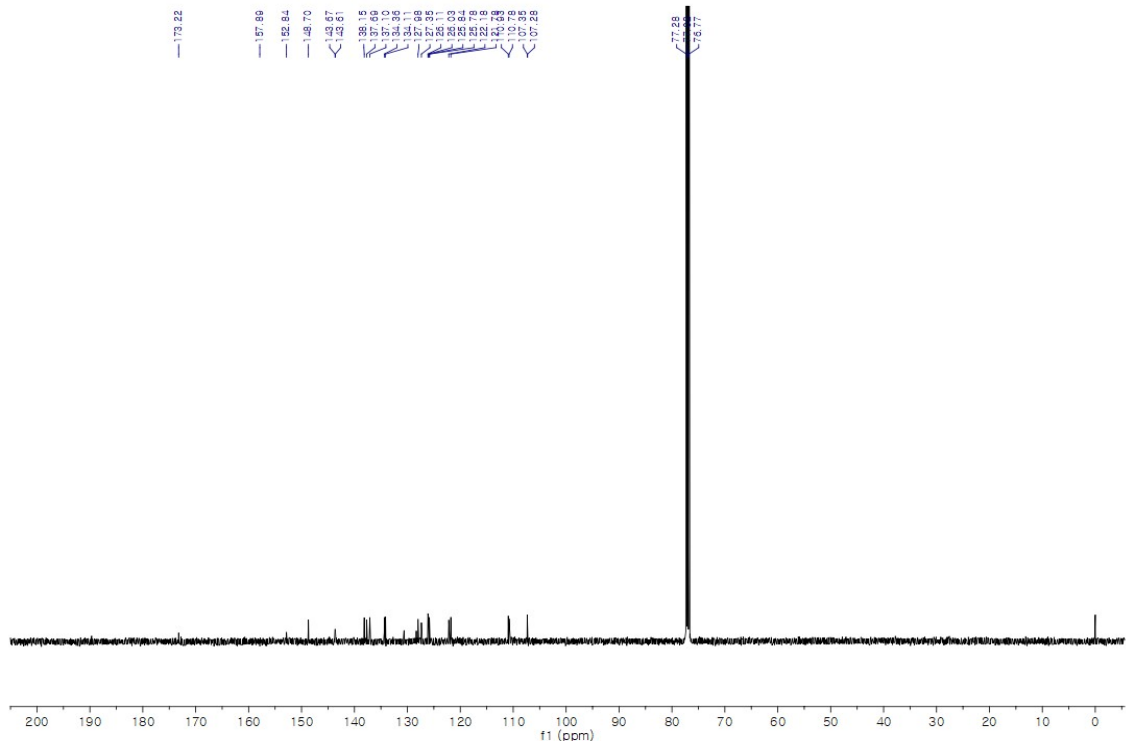
**Fig. S1.**  $^1\text{H}$ -NMR spectrum of  $\text{Ir}(\text{ppz})_3$  in  $\text{CDCl}_3$  (500 MHz, 293 K)



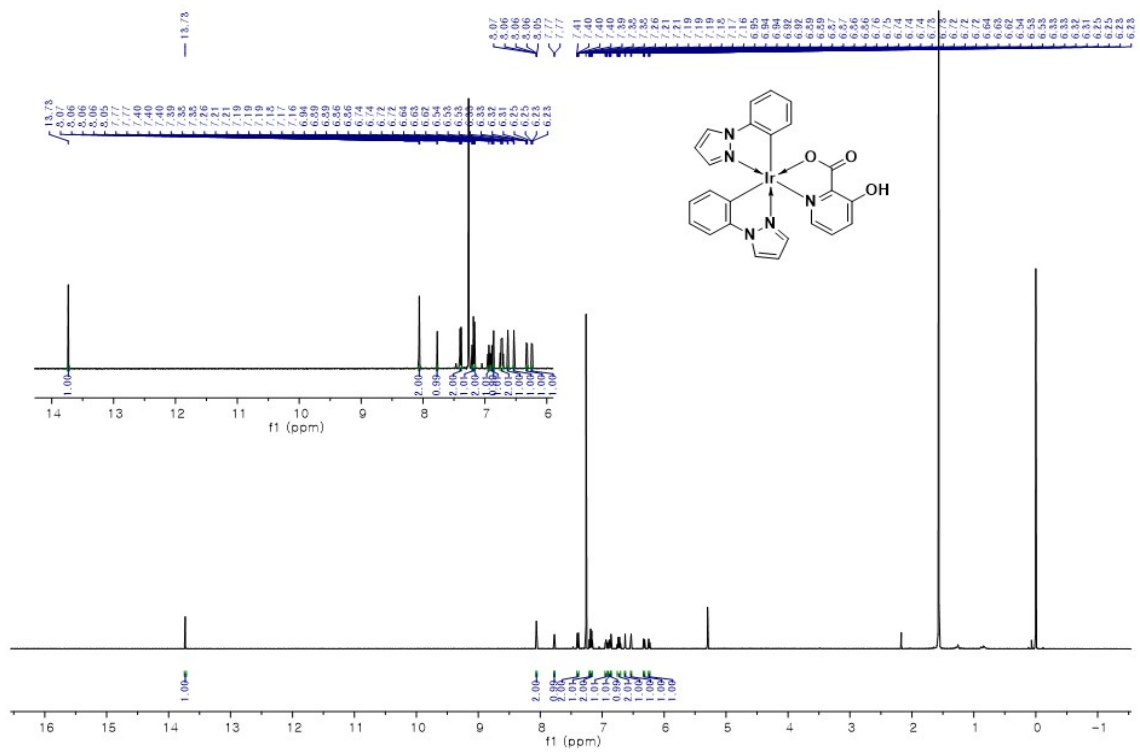
**Fig. S2.**  $^{13}\text{C}$ -NMR spectrum of  $\text{Ir}(\text{ppz})_3$  in  $\text{CDCl}_3$  (125 MHz, 293 K)



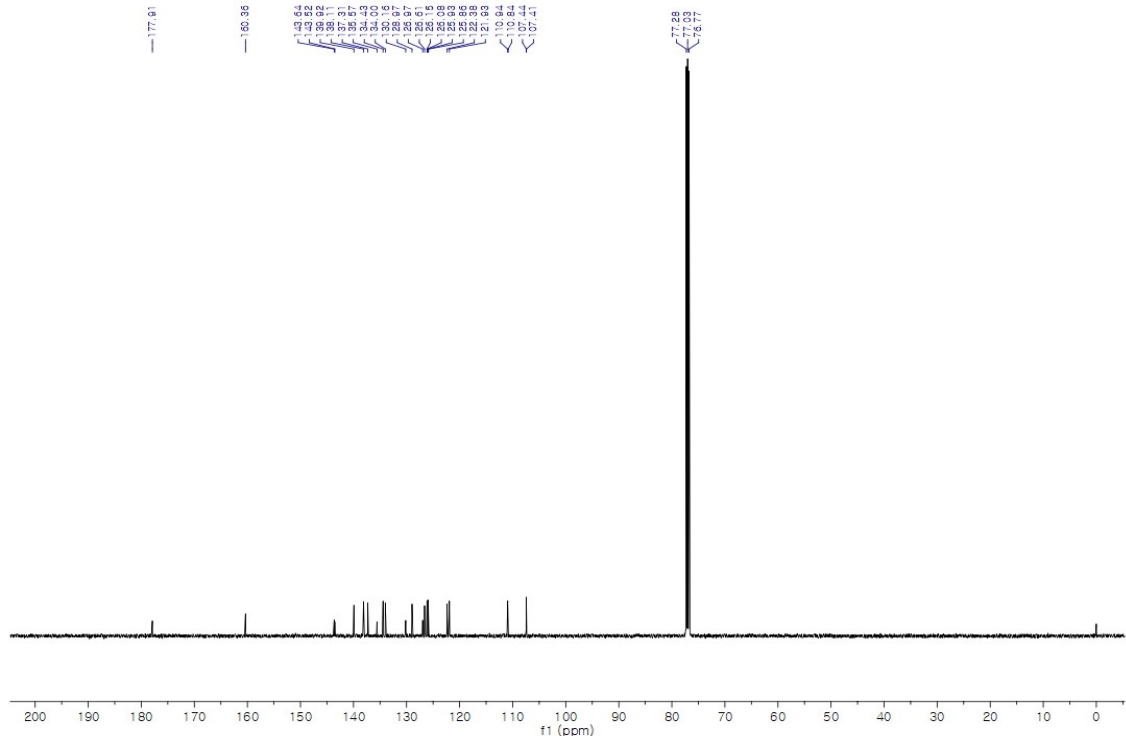
**Fig. S3.**  $^1\text{H}$ -NMR spectrum of  $\text{Ir}(\text{ppz})_2(\text{pic})$  in  $\text{CDCl}_3$  (500 MHz, 293 K)



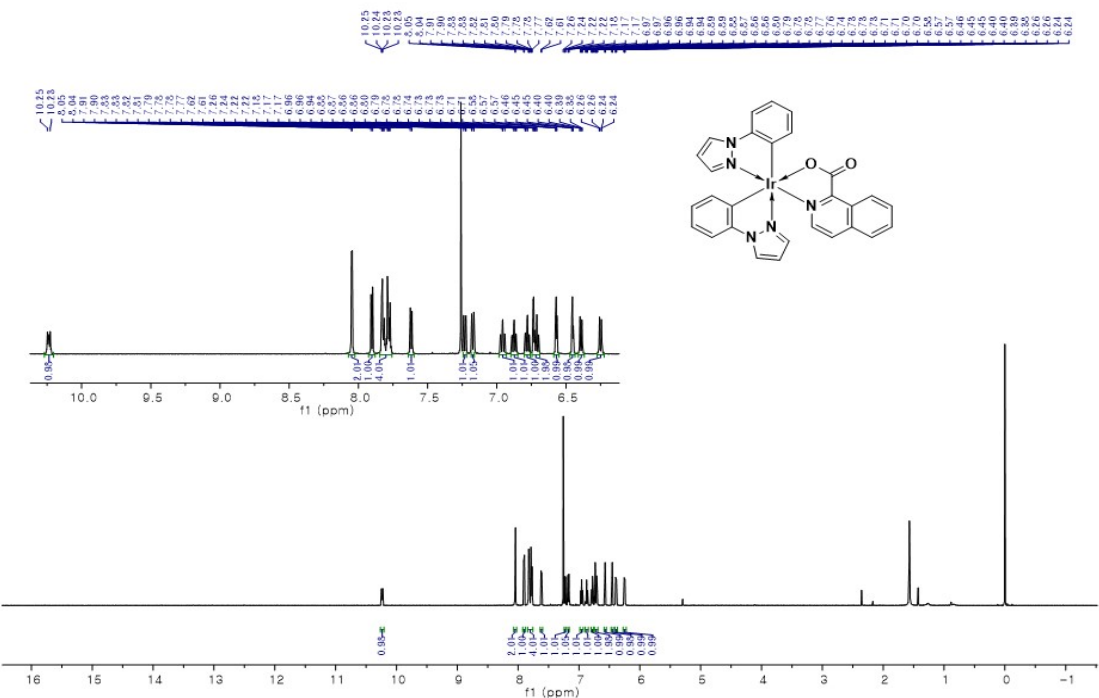
**Fig. S4.**  $^{13}\text{C}$ -NMR spectrum of  $\text{Ir}(\text{ppz})_2(\text{pic})$  in  $\text{CDCl}_3$  (125 MHz, 293 K)



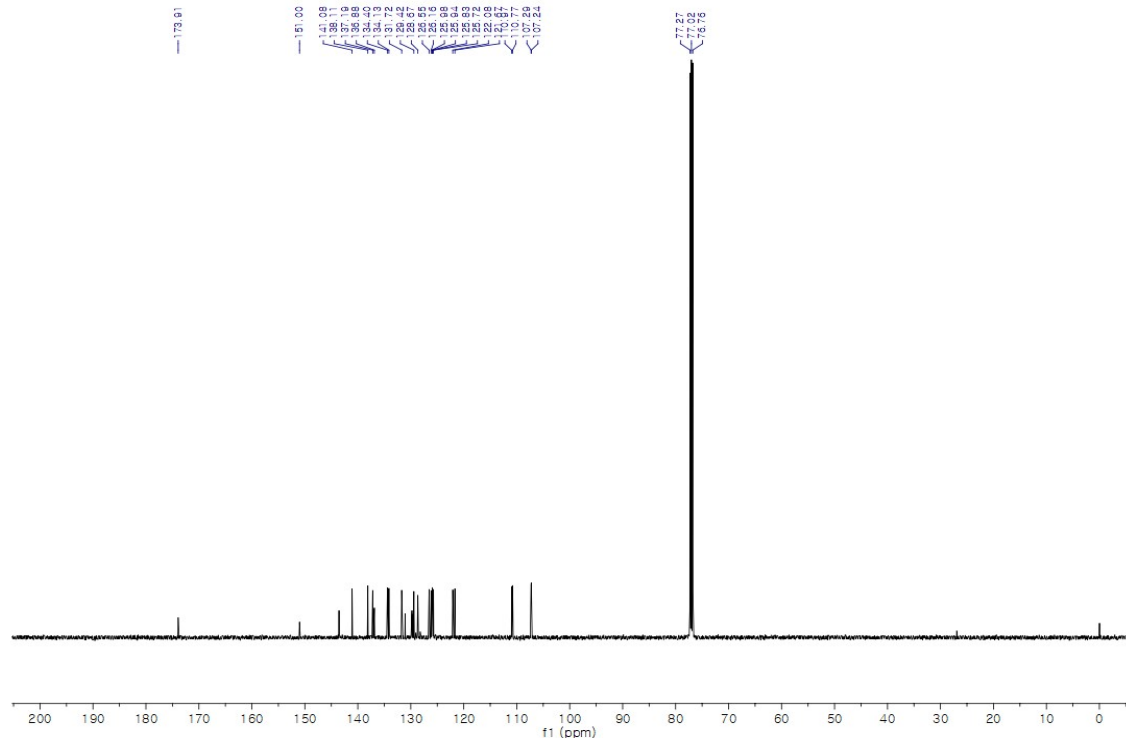
**Fig. S5.**  $^1\text{H}$ -NMR spectrum of  $\text{Ir}(\text{ppz})_2(\text{picOH})$  in  $\text{CDCl}_3$  (500 MHz, 293 K)



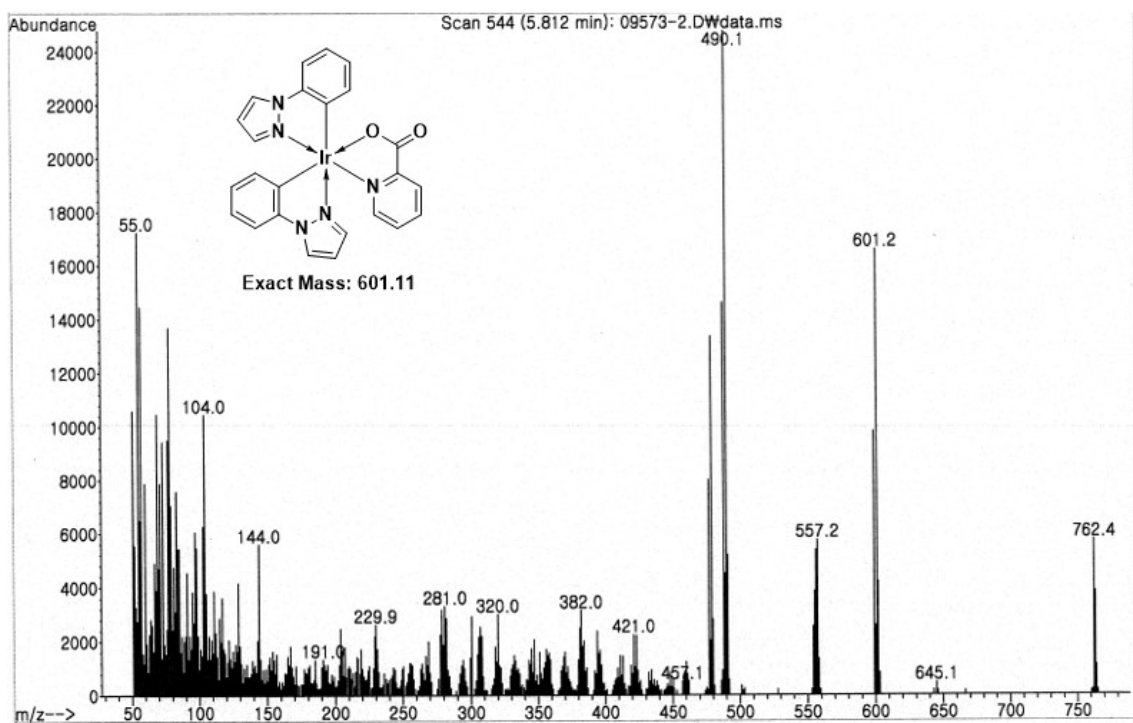
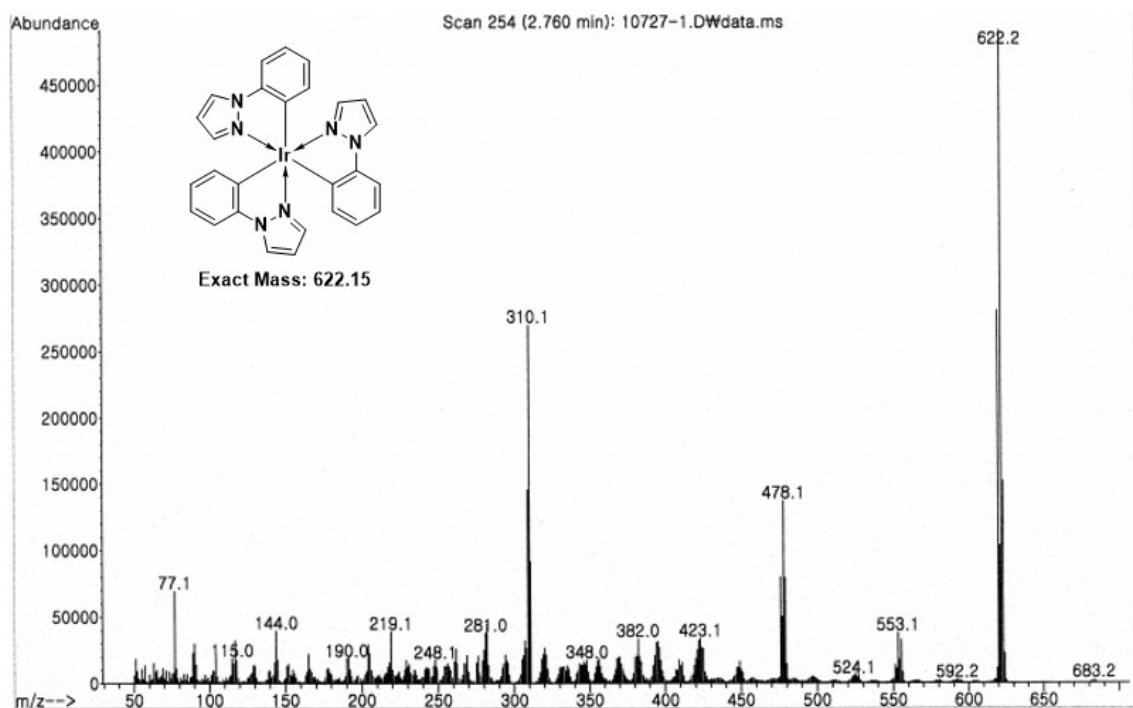
**Fig. S6.**  $^{13}\text{C}$ -NMR spectrum of  $\text{Ir}(\text{ppz})_2(\text{picOH})$  in  $\text{CDCl}_3$  (125MHz, 293K)



**Fig. S7.**  $^1\text{H}$ -NMR spectrum of  $\text{Ir}(\text{ppz})_2(\text{iq})$  in  $\text{CDCl}_3$  (500 MHz, 293 K)



**Fig. S8.**  $^{13}\text{C}$ -NMR spectrum of  $\text{Ir}(\text{ppz})_2(\text{iq})$  in  $\text{CDCl}_3$  (125 MHz, 293 K)



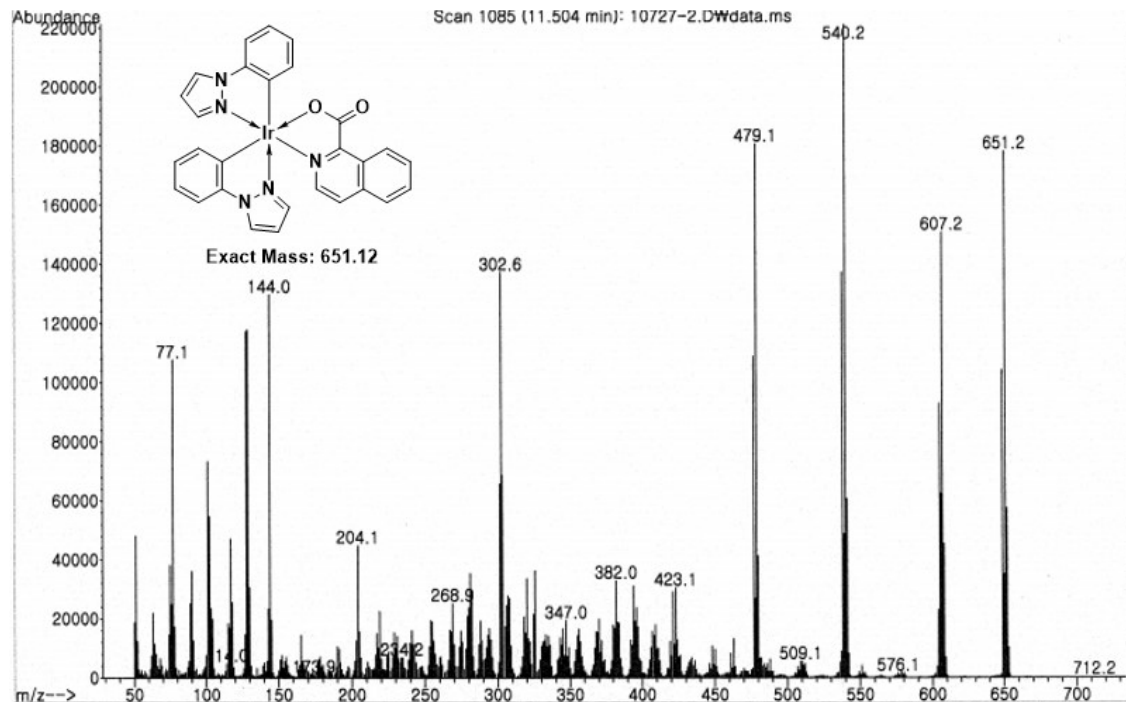
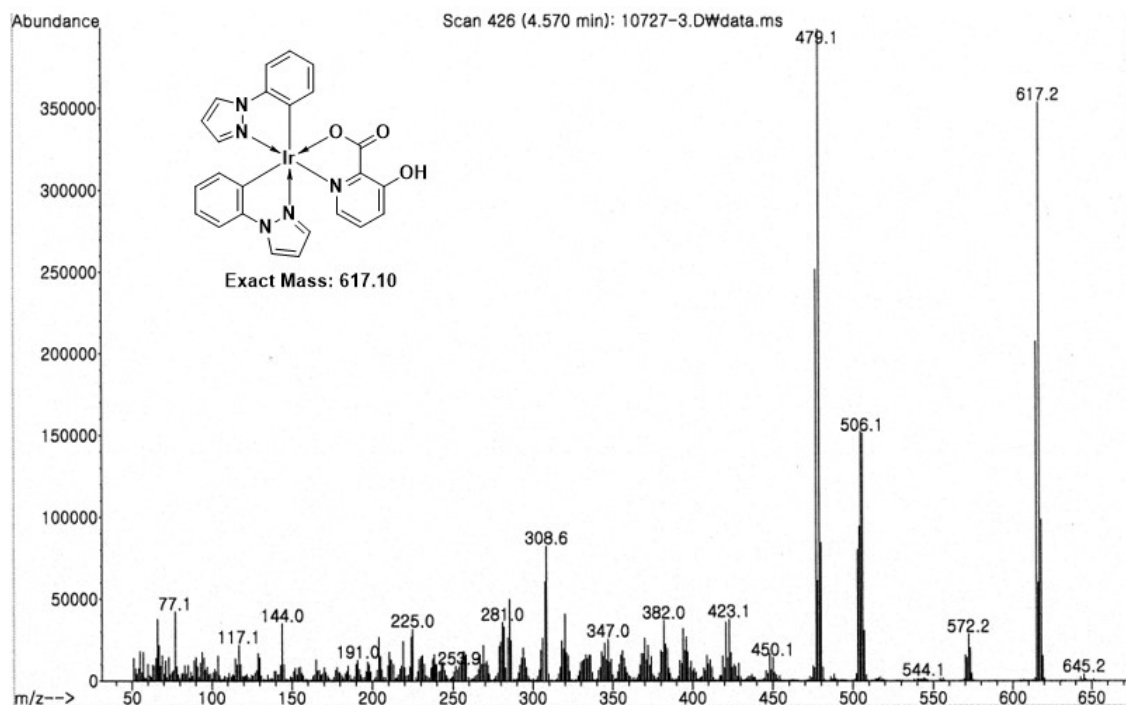


**Fig. S9.** GC-MS spectra of  $\text{Ir}(\text{ppz})_3$  and  $\text{Ir}(\text{ppz})_2(\text{LX})$

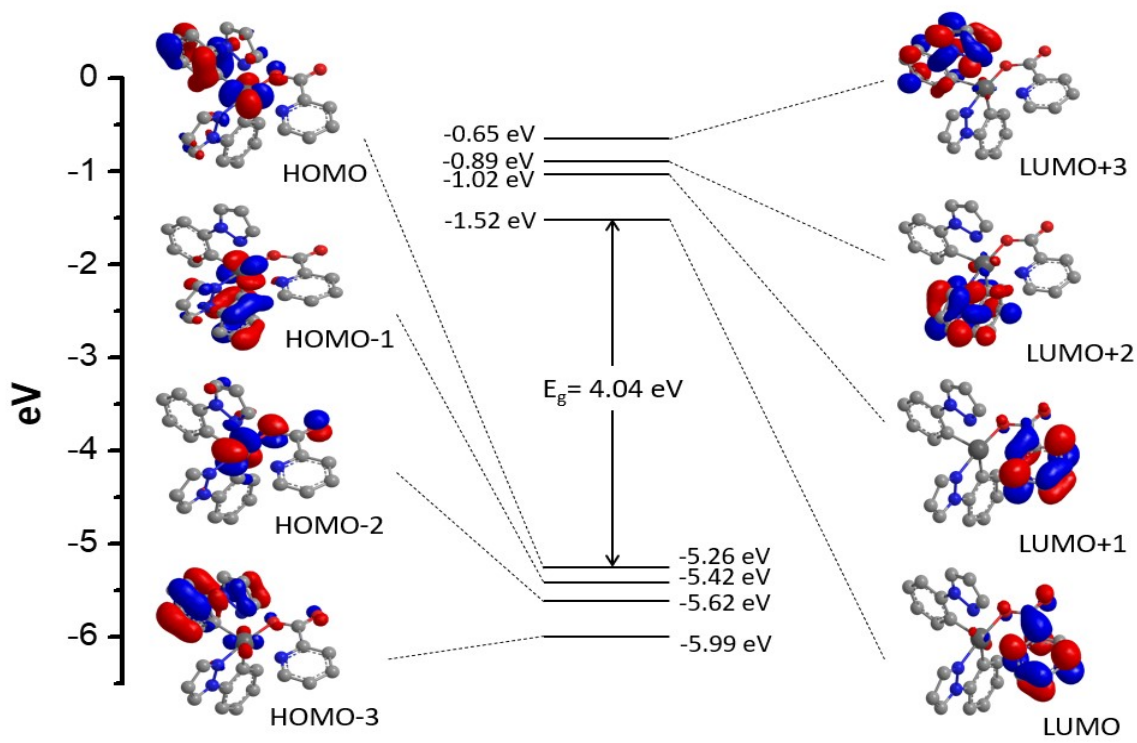


**Fig. S10.** Energy levels and isodensity plots (isodensity contour = 0.045 a.u.) for selected occupied and unoccupied molecular orbitals of  $\text{Ir}(\text{ppz})_2(\text{pic})$  obtained by DFT calculations.

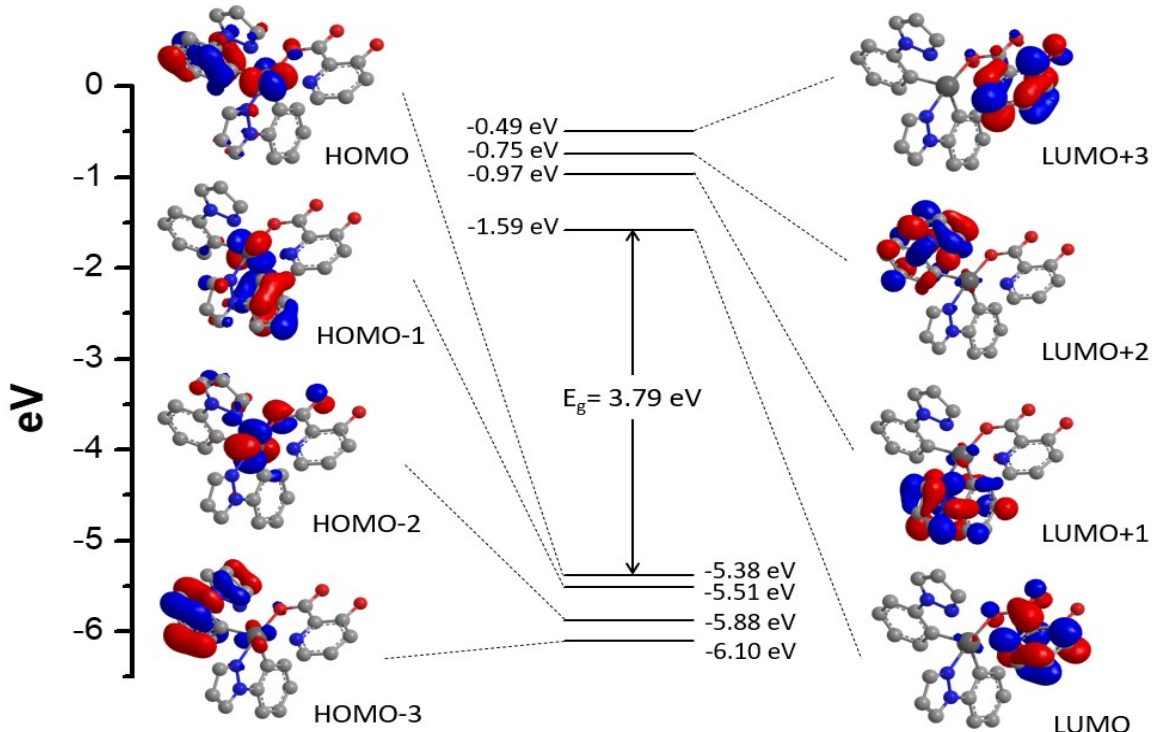


**Fig. S11.** Energy levels and isodensity plots (isodensity contour = 0.045 a.u.) for selected occupied and unoccupied molecular orbitals of  $\text{Ir}(\text{ppz})_2(\text{picOH})$  obtained by DFT calculations.

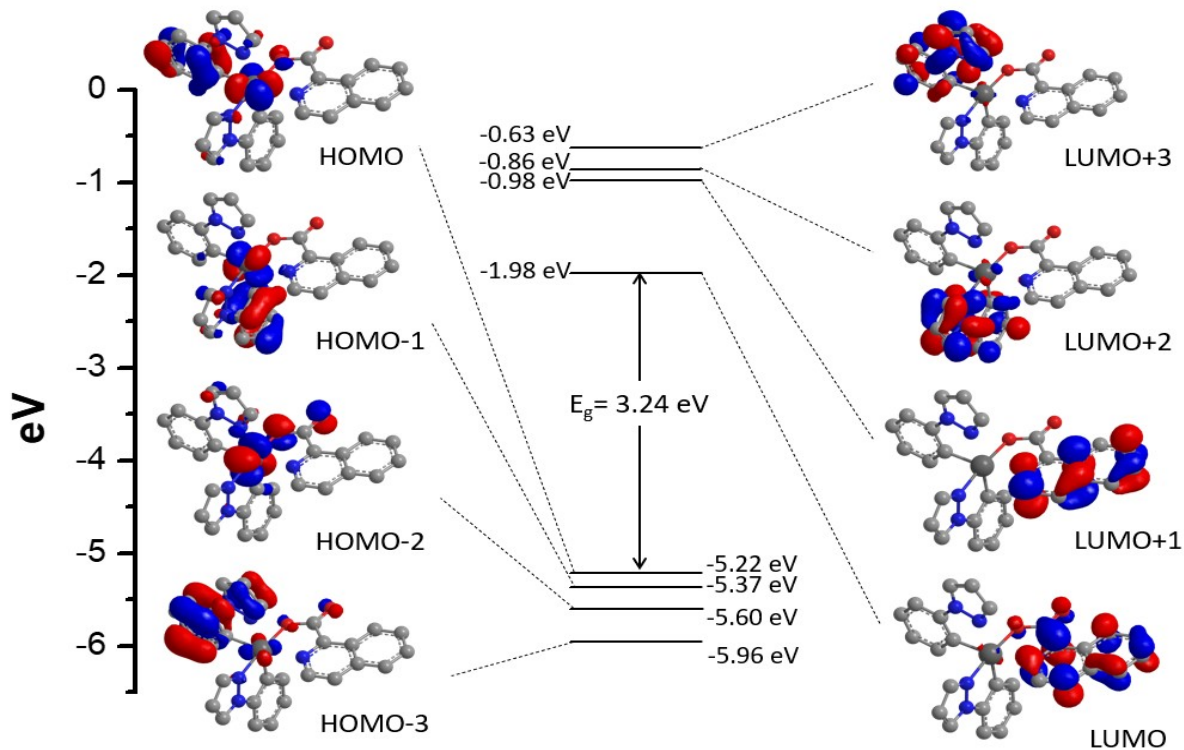


**Fig. S12.** Energy levels and isodensity plots (isodensity contour = 0.045 a.u.) for selected occupied and unoccupied molecular orbitals of  $\text{Ir}(\text{ppz})_2(\text{iq})$  obtained by DFT calculations.

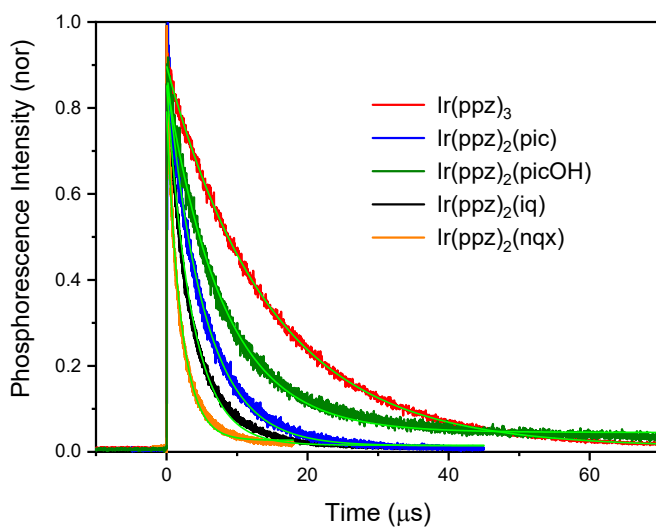


**Fig. S13.** Phosphorescence emission decay profiles for Ir complexes measured in MTHF matrix at 77 K ( $\lambda_{\text{ex}} = 355 \text{ nm}$ ).

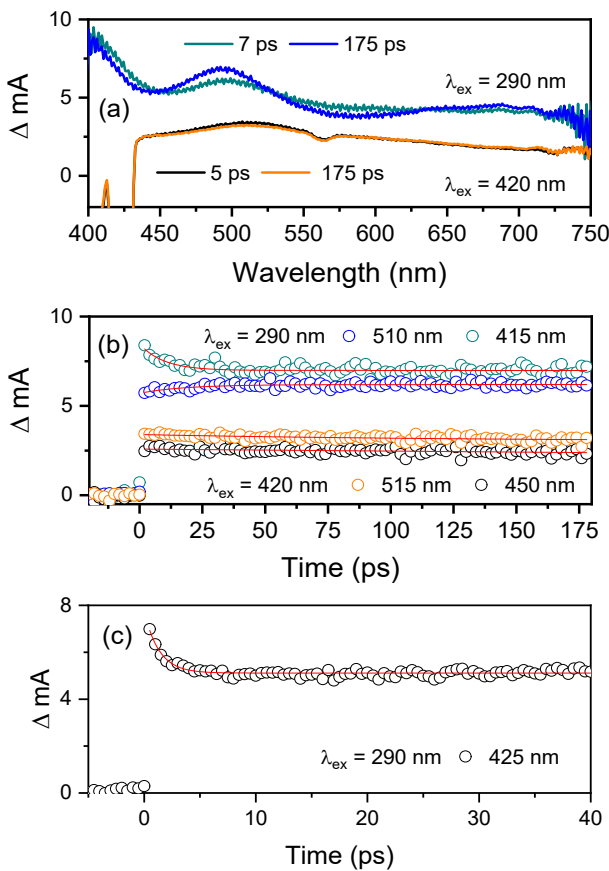


**Fig. S14.** (a) TA spectra of Ir(ppz)<sub>2</sub>(picOH) in the CH<sub>2</sub>Cl<sub>2</sub>-ethanol (v/v = 2:8) measured with time delays in the range of 5–175 ps, (b) corresponding decay profiles monitored at various wavelengths, and (c) the decay profile monitored at 425 nm. The excitation wavelengths were 290 and 420 nm, respectively. All TA spectra were chirp-corrected.

### femtosecond time-resolved TA measurements

fs-TA were carried out using a transient absorption spectroscopy system (Ultrafast Systems, Helios) equipped with a Ti:sapphire femtosecond laser system. The laser pulses were generated from the Ti:sapphire laser combination system, which consisted of a titanium sapphire laser (Spectra Physics, MaiTai SP) that was used to generate a seed pulse, and a regenerative amplified titanium sapphire laser system (Spectra Physics, Spitfire Ace, 1 kHz) pumped by a diode-pumped Q-switched laser (Spectra Physics, Empower). The excitation source (290, 350, and 420 nm) was an optical parametric amplifier (Spectra Physics, TOPAS prime). The probe source emitted white-light continuum pulses generated by focusing the 800 nm pulse onto a 1 mm path length quartz cuvette containing purified water. The pump-probe lights were directed to the sample cell with an optical path of 2 mm. The probe light was detected with a CCD detector installed in the absorption spectroscopy system after the controlled optical delay. The pump pulse was chopped by a mechanical chopper synchronised to one-half of the laser repetition rate, resulting in a pair of spectra with and without the pump, from which absorption changes induced by the pump pulse were estimated.

### TD-DFT calculation

Based on the optimized ground-state structures (Table S1-4), the absorption properties were calculated using a time-dependent DFT (TD-DFT) approach at an identical basis level. The vertical excitations at low energy were calculated to compare the experimental spectra. The 20 contributions of theoretical peaks with substantial oscillator strengths are listed in Table S5-8. The TD-DFT excitations were analysed with respect to the corresponding electronic transitions between occupied and unoccupied frontier MOs. The theoretical absorption peaks were assigned to LC and MLCT transitions, which were in good agreement with the experimental spectra (Fig. S15-S18).

**Table S1.** Cartesian coordinates for optimized structure for Ir(ppz)<sub>3</sub>

Atom	X	Y	Z	Atom	X	Y	Z
N	0.23159	1.346678	1.547865	C	-2.44222	-1.67623	-0.2063
C	-0.04185	3.41984	2.316977	C	-1.87668	-0.72792	0.671373
C	0.567133	2.683184	3.319112	C	-1.84311	-2.77451	-2.43235
N	-0.23351	2.590718	1.258616	C	-0.73387	-2.65376	-3.25409
C	-0.80972	2.763356	-0.02856	C	0.108868	-1.73437	-2.60807
C	-0.81762	1.594318	-0.82378	Ir	0.007656	-0.02872	0.052152
C	-1.37921	1.743542	-2.10314	H	-0.34812	4.452929	2.281104
C	-1.88982	2.965551	-2.54811	H	0.861467	3.033799	4.296113
C	-1.85937	4.094287	-1.72441	H	-1.41579	0.885964	-2.76876
C	-1.3122	3.995514	-0.44641	H	-2.3159	3.039038	-3.54555
C	0.71915	1.389166	2.792094	H	-2.25674	5.0434	-2.07077
N	2.471016	-1.58799	0.774155	H	-1.28059	4.865604	0.20329
C	2.478025	1.279047	-1.52002	H	1.146477	0.5012	3.231633
C	3.82556	1.344309	-1.88771	H	1.784225	2.002372	-1.94118
C	4.74316	0.428925	-1.36725	H	4.162449	2.110802	-2.58154
C	4.305663	-0.55164	-0.47842	H	5.791311	0.473336	-1.64815
C	2.95242	-0.58811	-0.13191	H	5.015058	-1.26821	-0.07389
C	1.984031	0.311966	-0.62705	H	4.165399	-2.7358	1.362667
N	1.142333	-1.59784	1.05555	H	2.307554	-4.09877	2.84892
C	3.102253	-2.58015	1.452373	H	-0.06449	-2.79457	2.27191
C	2.147245	-3.25427	2.196392	H	-2.27238	0.279766	2.533549
C	0.935573	-2.60094	1.912776	H	-4.44178	-0.81006	2.950023
N	-1.65285	-1.96485	-1.36081	H	-5.34848	-2.47293	1.335733
N	-0.45601	-1.32482	-1.46747	H	-4.06023	-3.03695	-0.70394
C	-2.64511	-0.44434	1.811945	H	-2.73821	-3.36709	-2.53385
C	-3.87742	-1.05981	2.054734	H	-0.5607	-3.15977	-4.19117
C	-4.39173	-1.99345	1.151473	H	1.073356	-1.34302	-2.89287
C	-3.66771	-2.31069	0.002586	H	1.073356	-1.34302	-2.89287

**Table S2.** Cartesian coordinates for optimized structure for Ir(ppz)<sub>2</sub>(pic)

Atom	X	Y	Z	Atom	X	Y	Z
N	-0.14776	-1.07295	1.617225	Ir	-0.04272	0.106668	-0.04731
N	0.438704	-2.29641	1.493903	C	0.31369	-2.99331	2.651251
C	1.03826	-2.5824	0.234558	C	-0.37669	-2.19487	3.549037
C	0.919913	-1.53967	-0.70876	C	-0.64724	-1.00267	2.856813

C	1.482412	-1.78553	-1.97031	C	-3.29038	2.709736	0.690388
C	2.124932	-2.99319	-2.25767	C	-2.4137	3.591522	1.30094
C	2.223471	-3.99803	-1.2901	C	-1.1629	2.953583	1.251611
C	1.67371	-3.79691	-0.02451	H	1.4023	-1.02061	-2.73676
C	-2.27625	-1.67727	-1.27586	H	2.549503	-3.15512	-3.24496
C	-3.60082	-1.93597	-1.63768	H	2.722703	-4.93502	-1.51729
C	-4.60643	-1.01068	-1.35274	H	1.740111	-4.57431	0.731469
C	-4.28079	0.177658	-0.70268	H	-1.51241	-2.40816	-1.52001
C	-2.94977	0.412736	-0.35361	H	-3.84828	-2.86314	-2.14796
C	-1.90025	-0.49355	-0.62199	H	-5.63679	-1.20742	-1.63301
N	-2.57764	1.618648	0.312804	H	-5.05717	0.903171	-0.47876
N	-1.27379	1.763139	0.656041	H	2.325065	0.297759	2.218443
C	2.673876	0.959007	1.431764	H	4.494722	1.529017	2.416327
C	3.877837	1.649403	1.532104	H	5.201234	3.035363	0.533077
C	4.266516	2.48491	0.481945	H	3.669202	3.220493	-1.48603
C	3.437163	2.596658	-0.63056	H	0.71531	-3.9892	2.750423
C	2.24654	1.873556	-0.66249	H	-0.65142	-2.44399	4.562226
N	1.875404	1.073392	0.357677	H	-1.17034	-0.11356	3.17411
C	1.308815	1.952398	-1.8608	H	-4.34842	2.786024	0.49791
O	0.242953	1.208297	-1.78382	H	-2.64759	4.560216	1.714718
O	1.612663	2.68291	-2.79642	H	-0.19941	3.291935	1.603414

**Table S3.** Cartesian coordinates for optimized structure for Ir(ppz)<sub>2</sub>(picOH)

Atom	X	Y	Z	Atom	X	Y	Z
N	0.792938	1.037482	1.562307	C	-2.69476	-0.84829	-0.37799
C	1.169778	3.019081	2.509322	N	-1.98198	-0.21248	0.572816
C	1.567891	2.045876	3.41193	C	-1.95785	-1.30212	-1.60427
N	0.707344	2.387466	1.40147	O	-0.69828	-1.04201	-1.66337
C	0.169711	2.83954	0.163357	O	-2.60334	-1.89603	-2.49353
C	-0.18792	1.799636	-0.72057	O	-4.76945	-1.71589	-1.18897
C	-0.70831	2.199177	-1.96038	Ir	0.126715	-0.06515	-0.01228
C	-0.86388	3.550437	-2.28308	H	1.183493	4.095404	2.574298
C	-0.50023	4.548394	-1.37378	H	1.987924	2.202628	4.393252
C	0.025686	4.19509	-0.13156	H	-0.98379	1.438066	-2.6842
C	1.31559	0.819629	2.774923	H	-1.26888	3.82883	-3.25238
N	1.922653	-2.41202	0.31459	H	-0.62221	5.596772	-1.62811
C	2.76811	0.678145	-1.47909	H	0.31616	4.963638	0.579137
C	4.060813	0.396289	-1.92854	H	1.482131	-0.19153	3.113278
C	4.661111	-0.82925	-1.63496	H	2.320621	1.634024	-1.73047
C	3.961656	-1.77454	-0.88791	H	4.600573	1.136116	-2.51375
C	2.671194	-1.46909	-0.45196	H	5.664941	-1.0525	-1.98322
C	2.024449	-0.24369	-0.72625	H	4.42128	-2.73089	-0.657
N	0.687635	-2.03545	0.729764	H	3.133401	-4.15393	0.495242
C	2.197798	-3.67337	0.732062	H	0.980988	-5.09252	1.911982
C	1.09942	-4.12774	1.443562	H	-0.8124	-2.99637	1.832327
C	0.179743	-3.06612	1.411123	H	-1.96043	0.731823	2.410242
C	-2.58546	0.2244	1.684159	H	-4.41669	0.396232	2.798314
C	-3.95553	0.029376	1.886965	H	-5.77778	-0.79458	1.050921
C	-4.7132	-0.6263	0.92714	H	-4.08619	-1.9269	-1.90803
C	-4.08111	-1.08314	-0.24361				

**Table S4.** Cartesian coordinates for optimized structure for Ir(ppz)<sub>2</sub>(iq)

Atom	X	Y	Z	Atom	X	Y	Z
N	1.286904	0.958548	1.554916	C	-1.69743	-1.04616	-1.68151
C	1.926546	2.886402	2.474105	O	-0.40199	-0.93372	-1.66698
C	2.164085	1.885798	3.402736	O	-2.33086	-1.57603	-2.58953
N	1.398863	2.303503	1.368346	C	-5.76967	0.192012	1.115293
C	0.957344	2.802836	0.110357	C	-6.62557	-0.34432	0.180975
C	0.475251	1.807775	-0.76644	C	-6.11174	-0.93519	-0.99814
C	0.043662	2.254387	-2.02453	C	-4.75599	-0.9866	-1.23581
C	0.088234	3.607781	-2.37107	Ir	0.506005	-0.07059	-0.02877
C	0.569762	4.561046	-1.46832	H	2.093718	3.950782	2.51932
C	1.013	4.159686	-0.20865	H	2.583729	2.001822	4.389919
C	1.750505	0.694977	2.782482	H	-0.3205	1.525431	-2.74214
N	1.951317	-2.63949	0.372055	H	-0.25173	3.922938	-3.3541
C	3.276757	0.286122	-1.40627	H	0.603358	5.611353	-1.74132
C	4.532258	-0.17605	-1.80925	H	1.393935	4.892428	0.497204
C	4.946768	-1.47004	-1.48896	H	1.765259	-0.32231	3.142672
C	4.097961	-2.30184	-0.76206	H	2.974876	1.292268	-1.67823
C	2.848216	-1.81629	-0.37307	H	5.188852	0.476187	-2.37916
C	2.386667	-0.51588	-0.67477	H	5.921171	-1.8335	-1.80098
N	0.768687	-2.09155	0.746056	H	4.412529	-3.3103	-0.5103
C	2.035139	-3.92357	0.802475	H	2.901419	-4.5315	0.596781
C	0.862648	-4.21516	1.480143	H	0.596343	-5.15044	1.94773
C	0.101229	-3.0362	1.414064	H	-0.88457	-2.82632	1.802319
C	-2.10997	0.640226	1.593761	H	-1.3744	1.040316	2.282117
C	-3.45465	0.699566	1.843179	H	-3.82086	1.161701	2.754914
C	-4.36722	0.157151	0.904384	H	-6.15194	0.649307	2.02377
C	-3.84144	-0.44087	-0.2898	H	-7.69891	-0.315	0.34562
C	-2.41886	-0.45221	-0.46064	H	-6.79846	-1.35419	-1.72771
N	-1.60956	0.071073	0.461868	H	-4.34797	-1.43434	-2.13187

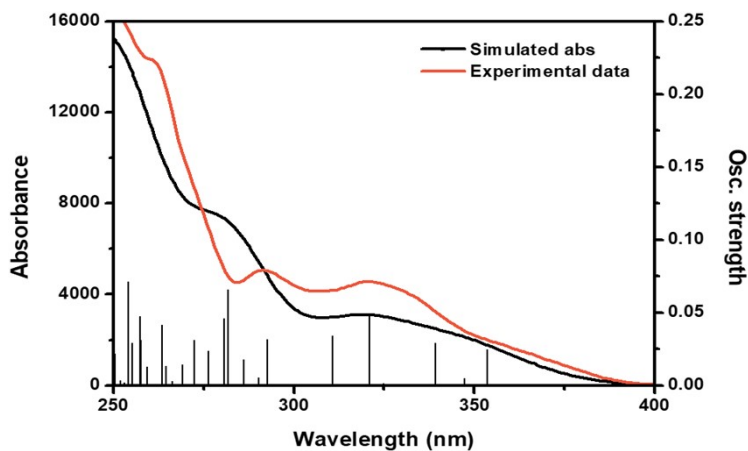


**Fig. S15.** Electronic transition and simulated absorption spectra of  $\text{Ir}(\text{ppz})_3$  in the ground state geometry obtained by TD-DFT calculations.

**Table S5.** TD-DFT calculation: Transition assignment of  $\text{Ir}(\text{ppz})_3$

No	Excitation Energy ( $\text{cm}^{-1}$ )	Wavelength (nm)	Oscillator strength	Assignment
1	28273.15424	353.692407827	0.0243	HOMO→LUMO (85%), HOMO→L+1 (13%)
2	28795.80512	347.272804435	0.0048	HOMO→LUMO (13%), HOMO→L+1 (83%)
3	29470.89584	339.317815593	0.0289	HOMO→L+2 (89%)
4	30782.3624	324.86135632	0.0015	H-1→LUMO (82%), H-1→L+1 (15%)
5	31157.4128	320.950910276	0.0478	H-1→LUMO (14%), H-1→L+1 (79%)
6	32175.29152	310.797494835	0.0339	H-1→L+2 (88%)
7	34156.20288	292.772590535	0.0314	H-3→LUMO (65%), H-2→LUMO (17%)
8	34459.46944	290.195994382	0.0051	H-3→L+1 (38%), H-3→L+2 (38%), H-2→LUMO (13%)
9	34945.82512	286.157215223	0.018	H-3→L+1 (13%), H-3→L+2 (43%), H-2→LUMO (20%)
10	35495.89904	281.72268545	0.0658	H-3→LUMO (19%), H-3→L+1 (25%), H-2→LUMO (15%)
11	35628.17488	280.676740632	0.046	H-3→L+1 (11%), H-2→LUMO (17%), H-2→L+1 (47%)
12	36175.02256	276.433828988	0.0234	H-2→L+2 (82%)
13	36723.48336	272.305323054	0.0313	HOMO→L+3 (80%)
14	37167.09136	269.055221544	0.0141	H-4→LUMO (79%)
15	37540.52864	266.378774148	0.0028	H-4→L+1 (69%)
16	37799.4344	264.554223065	0.0132	HOMO→L+4 (81%)
17	37943.80864	263.547607856	0.0413	H-4→L+2 (75%)
18	38566.47296	259.292572862	0.0126	H-6→LUMO (43%), H-5→LUMO (31%)
19	38807.6344	257.681256655	0.0311	H-6→L+1 (23%), H-5→L+1 (12%), H-1→L+3 (37%)
20	38852.80176	257.381695708	0.0475	H-6→LUMO (14%), H-5→LUMO (39%), HOMO→L+5 (10%)

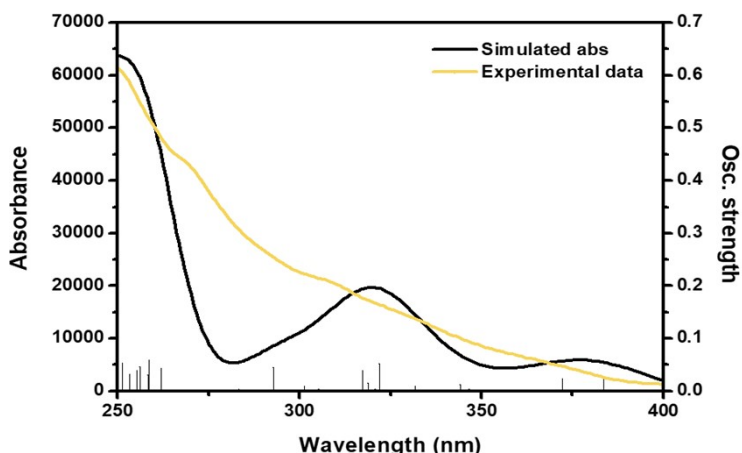


**Fig. S16.** Electronic transition and simulated absorption spectra of  $\text{Ir}(\text{ppz})_2(\text{pic})$  in the ground state geometry obtained by TD-DFT calculations.

**Table S6.** TD-DFT calculation: Transition assignment of  $\text{Ir}(\text{ppz})_2(\text{pic})$

No	Excitation Energy ( $\text{cm}^{-1}$ )	Wavelength (nm)	Oscillator strength	Assignment
1	24315.36432	411.262602048	0.0022	HOMO→LUMO (96%)
2	26063.9864	383.671163978	0.0273	H-1→LUMO (91%)
3	26862.4808	372.26643639	0.0232	H-2→LUMO (90%)
4	28853.87744	346.573871078	0.0034	HOMO→L+1 (80%), HOMO→L+2 (14%)
5	29061.96992	344.092297512	0.0123	H-1→L+2 (10%), HOMO→L+1 (16%), HOMO→L+2 (69%)
6	29721.736	336.454102143	0.0017	H-6→LUMO (3%), H-5→L+1 (2%), H-1→L+1 (2%)
7	30137.1144	331.816771416	0.0088	H-1→L+1 (94%)
8	31063.85184	321.917579684	0.0522	H-1→L+2 (39%), HOMO→L+3 (47%)
9	31175.96368	320.75993232	0.0042	H-2→L+1 (74%), H-2→L+2 (20%)
10	31364.69872	318.829780234	0.0145	H-2→L+1 (19%), H-2→L+2 (70%)
11	31523.59104	317.2227424	0.04	H-1→L+2 (37%), HOMO→L+3 (42%)
12	32117.2192	311.359459165	0.0001	H-5→LUMO (14%), H-3→LUMO (80%)
13	32771.33936	305.144684206	0.0031	H-1→L+3 (96%)
14	33177.03904	301.413275246	0.009	H-4→LUMO (97%)
15	34156.20288	292.772590535	0.0453	H-2→L+3 (88%)
16	34968.4088	285.972406042	0.0001	H-5→L+1 (59%), H-3→L+1 (31%)
17	35299.90496	283.286881688	0.0033	HOMO→L+4 (30%), HOMO→L+6 (51%)
18	36423.44304	274.548454659	0.0016	H-6→LUMO (43%), H-3→L+1 (33%)
19	36506.51872	273.923681321	0.0024	H-6→LUMO (30%), H-3→L+2 (55%)
20	36646.0536	272.880679299	0.0016	H-6→LUMO (16%), H-5→L+1 (17%), H-3→L+1 (29%)

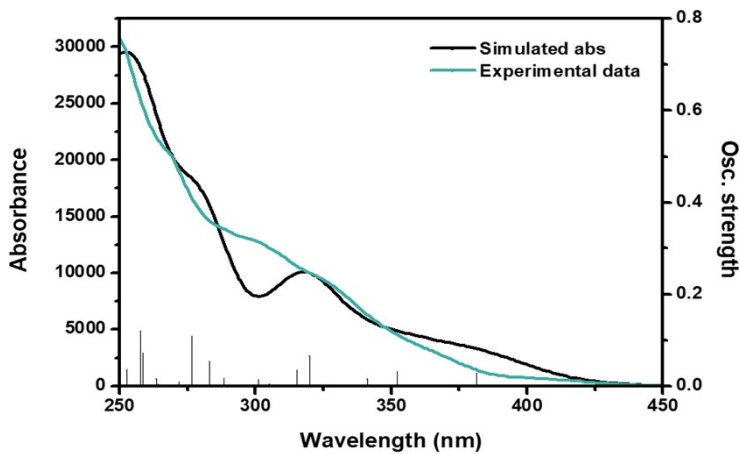


**Fig. S17.** Electronic transition and simulated absorption spectra of  $\text{Ir}(\text{ppz})_2(\text{picOH})$  in the ground state geometry obtained by TD-DFT calculations.

**Table S7.** TD-DFT calculation: Transition assignment of  $\text{Ir}(\text{ppz})_2(\text{picOH})$

No	Excitation Energy ( $\text{cm}^{-1}$ )	Wavelength (nm)	Oscillator strength	Assignment
1	24900.12032	401.604485098	0.0028	HOMO→LUMO (96%)
2	26223.68528	381.334655798	0.0279	H-1→LUMO (96%)
3	28394.9448	352.175363271	0.0317	H-2→LUMO (96%)
4	29312.00352	341.157164272	0.0145	H-1→L+1 (13%), HOMO→L+1 (83%)
5	31257.42624	319.923973369	0.0651	H-1→L+1 (49%), HOMO→L+2 (39%)
6	31716.35888	315.294704472	0.0352	H-1→L+1 (32%), HOMO→L+2 (52%)
7	32050.27472	312.009806074	0.0001	H-3→LUMO (88%)
8	32513.24016	307.567008111	0.0028	H-2→L+1 (90%)
9	32774.5656	305.114646584	0.0049	H-1→L+2 (92%)
10	33219.78672	301.025412483	0.0137	H-4→LUMO (95%)
11	33931.17264	294.714247164	0.0006	H-7→LUMO (37%), H-6→LUMO (45%)
12	34253.79664	291.938441309	0.0008	HOMO→L+3 (81%)
13	34674.82096	288.393702495	0.0164	H-5→LUMO (30%), H-1→L+3 (45%)
14	35030.51392	285.465409467	0.0034	H-1→L+3 (12%), HOMO→L+3 (10%), HOMO→L+4 (22%), HOMO→L+6 (33%)
15	35321.68208	283.112224875	0.0549	H-2→L+2 (78%)
16	36161.31104	276.538646205	0.1093	H-5→LUMO (51%), H-1→L+3 (37%)
17	36764.61792	272.000650782	0.0091	H-3→L+1 (90%)
18	37183.22256	268.938497298	0.0025	H-7→LUMO (16%), H-6→LUMO (12%), H-2→L+3 (18%), H-2→L+4 (12%), H-2→L+6 (30%)
19	37209.03248	268.751949016	0.0008	H-7→LUMO (36%), H-6→LUMO (29%), H-2→L+3 (18%)
20	37828.47056	264.351158055	0.0042	H-2→L+3 (60%), H-2→L+6 (19%)

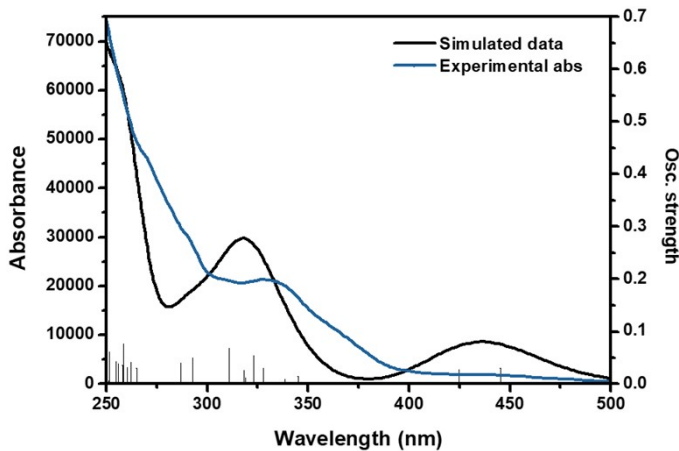


**Fig. S18.** Electronic transition and simulated absorption spectra of  $\text{Ir}(\text{ppz})_2(\text{iq})$  in the ground state geometry obtained by TD-DFT calculations.

**Table S8.** TD-DFT calculation: Transition assignment of  $\text{Ir}(\text{ppz})_2(\text{iq})$

No	Excitation Energy ( $\text{cm}^{-1}$ )	Wavelength (nm)	Oscillator strength	Assignment
1	20837.4776	479.904535086	0.002	HOMO $\rightarrow$ LUMO (96%)
2	22459.46976	445.246486531	0.0305	H-1 $\rightarrow$ LUMO (93%)
3	23541.06672	424.789586595	0.0278	H-2 $\rightarrow$ LUMO (93%)
4	26435.81056	378.274763972	0.0011	H-5 $\rightarrow$ LUMO (72%), H-3 $\rightarrow$ LUMO (20%)
5	28542.54528	350.354178364	0.0002	H-5 $\rightarrow$ LUMO (18%), H-3 $\rightarrow$ LUMO (77%)
6	28990.99264	344.934722456	0.0153	H-1 $\rightarrow$ L+2 (14%), HOMO $\rightarrow$ L+2 (81%)
7	29509.61072	338.872650503	0.0024	HOMO $\rightarrow$ L+1 (97%)
8	29534.61408	338.585768309	0.0094	H-4 $\rightarrow$ LUMO (98%)
9	30489.58112	327.980891592	0.0299	H-1 $\rightarrow$ L+1 (88%)
10	30958.99904	323.007859107	0.0536	H-1 $\rightarrow$ L+2 (40%), HOMO $\rightarrow$ L+3 (48%)
11	31349.37408	318.985635071	0.0124	H-2 $\rightarrow$ L+2 (68%), H-1 $\rightarrow$ L+2 (11%), HOMO $\rightarrow$ L+3 (11%)
12	31428.41696	318.183382024	0.0266	H-2 $\rightarrow$ L+2 (27%), H-1 $\rightarrow$ L+2 (27%), HOMO $\rightarrow$ L+3 (32%)
13	31882.51024	313.65158906	0.0008	H-2 $\rightarrow$ L+1 (98%)
14	32185.7768	310.696245181	0.0679	H-6 $\rightarrow$ LUMO (85%)
15	32589.86336	306.843876255	0.0039	H-1 $\rightarrow$ L+3 (96%)
16	32890.71024	304.037216802	0.003	H-7 $\rightarrow$ LUMO (90%)
17	34135.23232	292.952451773	0.0505	H-2 $\rightarrow$ L+3 (87%)
18	34868.39536	286.792664152	0.0395	H-8 $\rightarrow$ LUMO (63%), H-6 $\rightarrow$ L+1 (15%)
19	35423.30864	282.299999179	0.0037	HOMO $\rightarrow$ L+5 (28%), HOMO $\rightarrow$ L+7 (50%)
20	35474.92848	281.889222289	0.0019	H-9 $\rightarrow$ LUMO (78%), H-8 $\rightarrow$ LUMO (11%)